Available online at www.sciencedirect.com
SCIENCE DIRECT®
International Journal of Solids and Structures 42 (2005) 1729–1741
INTERNATIONAL JOURNAL OF SOLIDS and STRUCTURES
www.elsevier.com/locate/ijsolstr

Experimental and theoretical investigations of delamination at free edge of interface between piezoelectric thin films on a substrate

F. Shang [a,*], T. Kitamura [a], H. Hirakata [a], I. Kanno [b], H. Kotera [b], K. Terada [b]

[a] Department of Engineering Physics and Mechanics, Kyoto University, Yoshidahonmachi, Sakyoku, Kyoto 606-8501, Japan
[b] Department of Mechanical Engineering, Kyoto University, Yoshidahonmachi, Sakyoku, Kyoto 606-8501, Japan

Received 29 December 2003; received in revised form 9 August 2004
Available online 18 September 2004

Abstract

The interface strength of $Pb(Zr,Ti)O_3$ (PZT) thin films on a silicon substrate is studied experimentally and theoretically in this work. The focus is put on crack initiation from the free edge of the interface. A novel method of sandwiched cantilever specimen is utilized to perform the delamination tests. Theoretical analyses are performed on the singular behavior of the stress in the vicinity of the free edge along the interface between Cr layer and PZT layer, and on the distribution of normal stress at the delamination loads. Based on these results, a delamination criterion involving stress intensity parameter is adopted to estimate the interface toughness for crack initiation at the free edge along the interface Cr/PZT.

Keywords: Delamination; Thin film; Piezoelectric material; Interface strength

1. Introduction

Piezoelectric thin films, such as $Pb(Zr,Ti)O_3$ (PZT), are widely used in various functional devices applications such as nonvolatile random access memories (Scott and Araujo, 1989; Ramesh, 1997), micro-piezoelectric sensors and actuators in micro-electromechanical systems (MEMS) (Muralt et al., 1996; Muralt, 1997; Gardeniers et al., 1998; Kanno et al., 1998; Lee et al., 2000, 2003). These devices are often made from multi-layered thin films of dissimilar materials, which bring about a number of interfaces

* Corresponding author. Tel./fax: +81 75 753 5256.
E-mail address: shang@cyber.kues.kyoto-u.ac.jp (F. Shang).

0020-7683/$ - see front matter © 2004 Elsevier Ltd. All rights reserved.
doi:10.1016/j.ijsolstr.2004.08.004

and/or edges. Interfaces are intrinsic to these materials and have a special significance because they may just affect the structural performance of such materials and systems. However, they are susceptible to delaminate in the processing and in service. Especially, the delamination crack usually initiates at the free edge (intersection of the interface and the free-surface) of thin films due to the stress concentration originated from the mismatch of deformation (Evans and Hutchinson, 1995; Kinbara et al., 1998). In practice, delamination along the interface is found to be one of the major failure mechanisms occurred in various thin film/substrate systems (Kinbara et al., 1998; Volinsky et al., 1999; Lane et al., 2000; Kitamura et al., 2002). Another challenge concerning the structural integrity and reliability comes from the brittle nature of piezoelectric ceramics (Zhang et al., 2002). Therefore, it is of critical importance to evaluate the interface strength between the thin films on a substrate.

Recently, an experimental method of sandwiched cantilever was developed for evaluating the mechanical strength of interface between thin films (Kitamura et al., 2002). In the proposed method, plastic deformation and fracture of films are avoided by the sandwiched structure of specimen during the delamination tests. Therefore, it is able to eliminate the ambiguity of mechanical strength obtained by previous evaluation methods, such as scratch test, pull/topple test, peeling test and bending test. The validity and applicability of this method were shown for the thin films used in different applications fields (Kitamura et al., 2003; Hirakata, 2003).

In the present study, this sandwiched cantilever-testing scheme will be utilized to explore the interface strength of PZT thin films deposited on silicon substrate. Further, theoretical analyses will be conducted on the singular behavior of the stress in the vicinity of the free edge of interface. Based on these, interface toughness for crack initiation will be discussed.

2. Testing materials and experimental method

2.1. Preparation of PZT thin films

A ceramic target with a composition of $Pb(Zr_{0.53},Ti_{0.47})O_3$ was sputtered. After sputtering a thin Ti adhesion layer on a single-crystal silicon (Si) substrate with thickness of 520 μm followed by a Pt layer of 100 nm, $(Pb_{1-x}La_x)TiO_3$ (PLT) with $x = 0$–30% was deposited at 750 °C. The PZT layer was then sputtered at 700 °C with 180 W rf power by radio-frequency (rf) magnetron sputtering technique (Kanno et al., 1997; Kanno et al., 2003). The resulting thickness of the PZT film was approximately 2.5 μm, which is typical from the viewpoint of MEMS applications as micro-piezoelectric devices. Lastly, a chromium (Cr) layer of thickness of around 0.2 μm was deposited on the top surface of PZT layer. A final sequence, i.e., Cr/PZT/PLT/Pt/Ti/Si, was obtained for all the specimens tested in this study. The typical deposition conditions for fabricating these experimental specimens, as well as their geometries, are listed in Table 1. X-ray diffraction (XRD) tests show that the deposited PZT films were oriented in the axis of (0 0 1), see Fig. 1.

2.2. Experimental method

The experimental setup of the sandwiched cantilever-testing scheme is schematically shown in Fig. 2. The load, P, is applied at the edge of the cantilever of stainless steel. The interface delamination is expected to initiate at the left end, i.e., ''Edge'' in the figure, where the tensile stress concentrates. The relatively stiff steel cantilever and silicon substrate are chosen to constrain plastic deformation of the films during the tests. A square plate of film/substrate is cut from the wafer with PZT films and carefully glued with standard epoxy on the lower surface of cantilever. To achieve a better cohesive adhesive bonding strength all of the specimens were cured at 60 °C for 4 h.

Table 1
Growth conditions of the PZT films on silicon substrate

Target	$Pb(Zr_{0.53},Ti_{0.47})O_3$
Temperature	700/750 °C
Deposition rate	17–20 nm/min
Gas	Ar/O_2
Pressure	9.5/0.5 SCCM
RF power	180 W
Thickness	Cr/PZT/PLT/Pt/Ti/Si: 0.2/2.5/0.02/0.1/0.02/520 μm

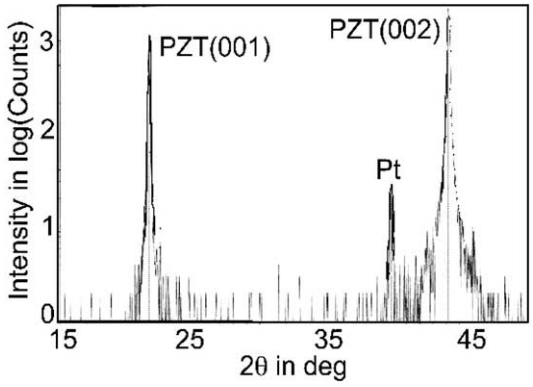

Fig. 1. X-ray diffraction profile of the PZT thin films.

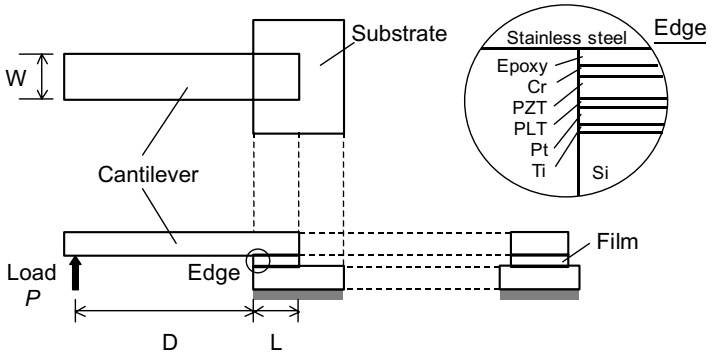

Fig. 2. Schematics of the specimen and loading system.

Table 2 lists the specimen sizes tested. A micro-material testing system, MCTE-500 (Shimadzu), is used to perform the tests. Tests are conducted in an air at a room temperature under the constant loading rate of 0.004 N/s using a remodeled micro-Vickers hardness tester with a maximum load capacity of 5 N. The load, P, is applied by an electro-magnetic actuator and the displacement at the loading point, δ, is measured continuously by means of a linear variable differential transformer during the tests. After the tests, the fracture surface is observed by means of an optical microscope, and the elements on the surface are examined by Auger electron spectroscopy (AES).

Table 2
Dimensions of the specimens of the PZT films

Test	L (mm)	W (mm)	D (mm)
D1	1.260	1.746	10
D2	1.484	1.725	10
D3	1.535	1.952	10

3. Experimental results

Table 3 lists the delamination load, P_d, and the delamination positions of the typical tests for the specimens of the PZT films.

Fig. 3 shows the load–displacement curves of the specimens up to the delamination. A linear relationship between the load P and the displacement δ is shown for all the specimens.

The fractographs in all of the tests examined by the optical microscope indicate that the fracture surfaces are smooth and flat on both of the cantilever and substrate sides, and the two sides show different gloss. To determine exactly the positions of crack initiation, AES was used to examine the elements on the surfaces of the fractured specimens that are immediately close to the free edges. Fig. 4a and b display the spectrum of Auger electron at these regions on the cantilever side and substrate side of the specimens, respectively. It is noted that the extra elements nitrogen and oxygen exist on the surfaces of the specimens. This might be attributed to that atmospheric contamination changed the surface condition irrevocably after fracture, which could occur in the AES analysis, according to Bubert and Jenett (2002). It is found that the Cr film

Table 3
Delamination load and fracture interface

Test	Delamination load P_d, N	Fracture interface
D1	1.294	Cr/PZT
D2	1.576	Cr/PZT
D3	2.136	Cr/PZT

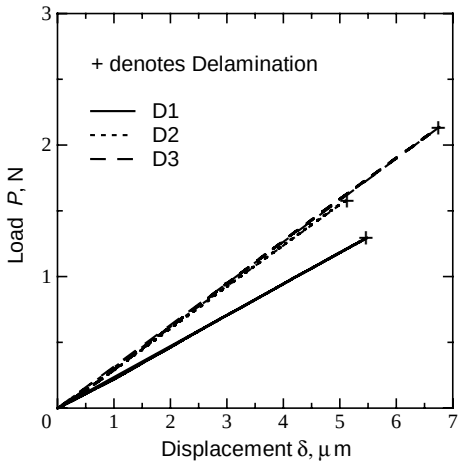

Fig. 3. Load–displacement curves of the specimens of the PZT films.

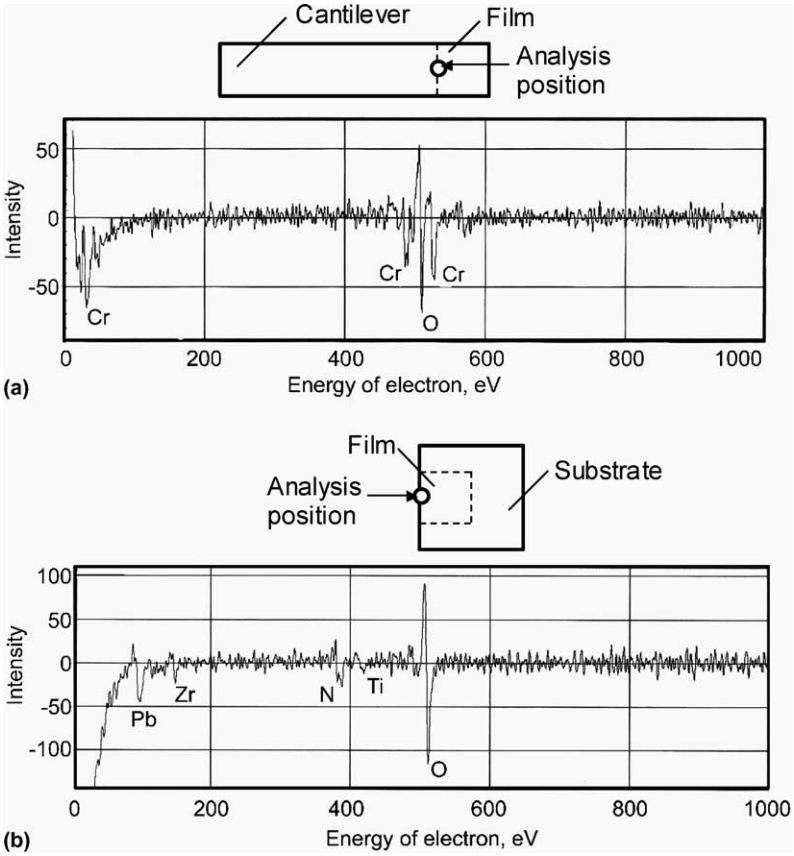

Fig. 4. Spectrum of Auger electron on the fracture surfaces: (a) cantilever side, and (b) substrate side.

covers the surface of the cantilever side, while the PZT layer remains on the surface of the substrate side of the specimen.

The above experimental results reveal that: (1) the delamination initiates at the free edge on the interface between the thin Cr layer and PZT layer. (2) Fracture occurs abruptly after the initiation and no evidence of slow stable crack growth show in all the tests. Therefore, the fracture is brittle of nature. Meanwhile, the results imply that strong stress intensification prevails over the region near the free edge of the interface and the delamination could be controlled by the parameter such as stress-intensity factor at the interface edge. Therefore, discussed next is the behavior of the stress field near the free edge along the interface Cr/PZT.

4. Stress field

Since the delamination occurred at the free edge along the interface between non-piezoelectric Cr layer and piezoelectric PZT layer, this section is devoted to a theoretical analysis for the stress field in the vicinity of the free edge along the interface Cr/PZT.

It is generally known that the stresses near the free edge of the interface in an isotropic elastic bi-material exhibit an r^{δ} behavior, where r is the radial distance from the edge and δ is the parameter with $0 < \mathrm{Re}(\delta) < 1$ (Williams, 1952; Bogy, 1968, 1971; Hein and Erdogan, 1971). For instance, the characterize equations

derived by Bogy (1968) give $\delta \leqslant 0.02$ for Pt/Ti interface edge. In comparison with the isotropic elastic materials, piezoelectric medium is usually anisotropic and requires alternative techniques to treat the electro-elastic problem. Wang and Zheng (1995) and Ding et al. (1996) found similar theoretical general solutions for piezoelectric materials by employing potential function method. Xu and Mutoh (2001) analyzed the stress fields at the interface edge of bonded transversely isotropic piezoelectric dissimilar materials under torsion loading and axisymmetric deformation, and the stress singularity was found. Li et al. (2002) also examined the problem under axisymmetric deformation and show that stress singularity existed at the bond edge. Nevertheless, the electro-elastic problems of the interface edge consisting of piezoelectric layers are not fully investigated. In this section, a new solution will be worked out for the interface edge problem involved.

4.1. Problem statement

Considering the sandwiched cantilever specimen and the materials of the Cr and PZT thin films, a two-dimensional model of linear elasticity and piezoelectricity can be adopted. The PZT film is transversely isotropic with the poling direction (i.e., positive z-axis) perpendicular to the isotropic plane (x–y plane). The Cr layer is assumed to be homogenous, linear elastic and isotropic with Lamé constants λ, μ and Poisson's ratio v. The x–z plane is assumed to be the plane of analysis. Let (r,θ) be local polar coordinates of a point with rectangular Cartesian coordinates (x,z) in the vicinity of the interface edge, see Fig. 5. Denote the two dimensional regions occupied by the Cr and PZT layers by D', D''. Suppose they share one straight segment B of their boundaries, and denote their remaining straight boundary segments by B', B''.

The equilibrium equations for piezoelectric materials take the form

$$\sigma_{ij,j} = 0, \quad D_{i,i} = 0 \tag{1}$$

where σ_{ij} and D_i are the stresses and electric displacements.

The boundary and interface conditions of interest can be expressed, in the local coordinate system (r,θ), as

$$\begin{aligned} &\sigma^1_{\theta\theta} = \sigma^1_{r\theta} = 0 \quad \text{on } B' \\ &\sigma^2_{\theta\theta} = \sigma^2_{r\theta} = D^2_{\theta} = 0 \quad \text{on } B'' \end{aligned} \tag{2a}$$

$$\sigma^1_{\theta\theta} = \sigma^2_{\theta\theta}, \quad \sigma^1_{r\theta} = \sigma^2_{r\theta}, \quad D^2_{\theta} = 0, \quad u^1_r = u^2_r, \quad u^1_{\theta} = u^2_{\theta} \quad \text{on } B \tag{2b}$$

Here, the superscripts 1 and 2 refer to the quantities associated with the Cr layer and the PZT layer, respectively. Since the goal of this analysis is to find the eigenequations determining the stress singularity near the

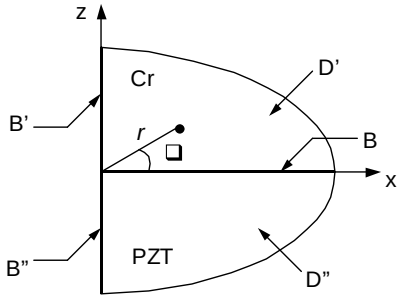

Fig. 5. Geometry of bonded Cr/PZT interface edge problem.

interface edge, no mechanical tractions and electrical loads are applied on the external boundaries. Electrically open boundary condition is adopted. Further, the continuity conditions at the interface are assumed.

4.2. Solution method

The piezoelectric interface edge problem can be solved with the aid of the general solution that has been obtained firstly by Wang and Zheng (1995) and further revised by Shang et al. (2003). In this framework, the displacements u_i and electric potential φ can be expressed by three potential functions ψ_i as

$$\begin{aligned} u_x &= (\psi_1 + \psi_2 + \psi_3)_{,x} \\ u_z &= (k_{11}\psi_1 + k_{12}\psi_2 + k_{13}\psi_3)_{,z} \\ \varphi &= (k_{21}\psi_1 + k_{22}\psi_2 + k_{23}\psi_3)_{,z} \end{aligned} \tag{3}$$

which has the form, in the coordinate system (r,θ), of

$$\begin{aligned} u_r &= \sum_{i=1}^{3}\left[(\cos^2\theta + k_{1i}\sin^2\theta)\cdot\psi_{i,r} + (k_{1i}-1)\sin\theta\cos\theta\cdot\psi_{i,\theta}/r\right] \\ u_\theta &= \sum_{i=1}^{3}\left[(k_{1i}-1)\sin\theta\cos\theta\cdot\psi_{i,r} + (k_{1i}\cos^2\theta + \sin^2\theta)\cdot\psi_{i,\theta}/r\right] \\ \varphi &= \sum_{i=1}^{3} k_{2i}[\sin\theta\cdot\psi_{i,r} + \cos\theta\cdot\psi_{i,\theta}/r] \end{aligned} \tag{4}$$

The solution requires that the potential functions satisfy the following relations

$$\psi_{i,xx} + \psi_{i,zz}/s_i^2 = 0, \quad i = 1,2,3 \tag{5}$$

or equivalently,

$$\psi_{i,r_ir_i} + \psi_{i,r_i}/r_i + \psi_{i,\theta_i\theta_i}/r_i^2 = 0, \quad i = 1,2,3 \tag{6}$$

In Eqs. (5) and (6), $r_i = r\cos\theta/\cos\theta_i$, $\theta_i = \arctan(s_i\tan\theta)$ and s_i $(i = 1,2,3)$ are the eigenvalues of the material constants. The detailed expressions of k_{ij} and s_i are given out in Wang and Zheng (1995) and Shang et al. (2003).

A general form of solutions satisfying Eq. (6) may be expressed as

$$\psi_i = \sum_{j=0}^{\infty}(r_i)^{p+j+1}\left[A_{ij}\sin(p+j+1)\theta_i + B_{ij}\cos(p+j+1)\theta_i\right], \quad i = 1,2,3 \tag{7}$$

where $0 < p < 1$, A_{ij} and B_{ij} are constants. Then, according to the constitutive relations of linear piezoelectric materials, the stresses and electric displacements can be expressed by

$$(\sigma_{rr},\sigma_{\theta\theta},\sigma_{r\theta})^{\mathrm{T}} = \mathbf{A}\mathbf{B}_1\mathbf{C}\left(\sum_{i=1}^{3}\mathbf{\Lambda}_{1i}\mathbf{E}_i, \sum_{i=1}^{3}\mathbf{\Lambda}_{2i}\mathbf{E}_i\right)^{\mathrm{T}} \tag{8}$$

$$(D_r, D_\theta)^{\mathrm{T}} = \mathbf{D}\mathbf{B}_2\mathbf{C}\left(\sum_{i=1}^{3}\mathbf{\Lambda}_{1i}\mathbf{E}_i, \sum_{i=1}^{3}\mathbf{\Lambda}_{2i}\mathbf{E}_i\right)^{\mathrm{T}} \tag{9}$$

The detailed expressions of the matrices $\mathbf{A}$, $\mathbf{B}_1$, $\mathbf{B}_2$, $\mathbf{C}$, $\mathbf{E}_i$ and the vectors $\mathbf{\Lambda}_{1i}$, $\mathbf{\Lambda}_{2i}$ are listed in Appendix A.

For the case of the elastic Cr layer, the solution can be readily constructed by modifying the known Boussinesq's solution (Timoshenko and Goodier, 1987),

$$\begin{pmatrix} 2\mu u_x \\ 2\mu u_z \end{pmatrix} = \begin{pmatrix} (\phi_1 + z\phi_2)_{,x} \\ (\phi_1 + z\phi_2)_{,z} - 4(1-\nu)\phi_2 \end{pmatrix} \tag{10}$$

Here ϕ_i $(i = 1, 2)$ are arbitrary functions satisfying two-dimensional Laplacian equations. By applying the coordinate transformation from (x, z) to (r, θ), one arrives at

$$\begin{pmatrix} 2\mu u_r \\ 2\mu u_\theta \end{pmatrix} = \begin{pmatrix} (\phi_1 + r\sin\theta\phi_2)_{,r} \\ (\phi_1 + r\sin\theta\phi_2)_{,\theta}/r - 4(1-\nu)\cos\theta\phi_2 \end{pmatrix} \tag{11}$$

And the stresses are given by

$$\begin{pmatrix} \sigma_{rr} \\ \sigma_{\theta\theta} \\ \sigma_{r\theta} \end{pmatrix} = \mathbf{B}_3 \begin{pmatrix} (\phi_1 + r\sin\theta\phi_2)_{,rr} \\ \left[(\phi_1 + r\sin\theta\phi_2)_{,r} - 4(1-\nu)(\cos\theta\phi_2)_{,\theta}\right]/r + (\phi_1 + r\sin\theta\phi_2)_{,\theta\theta}/r^2 \\ \left[(\phi_1 + r\sin\theta\phi_2)_{,r\theta} + 2(1-\nu)\cos\theta(\phi_2 - r\phi_{2,r})\right]/r - (\phi_1 + r\sin\theta\phi_2)_{,\theta}/r^2 \end{pmatrix} \tag{12}$$

The matrix $\mathbf{B}_3$ is also listed in Appendix A. Similar to the form of solutions Eq. (7), the functions ϕ_i can be written as

$$\phi_i = \sum_{j=0}^{\infty} r^{p+j+1}\left[C_{ij}\sin(p+j+1)\theta + D_{ij}\cos(p+j+1)\theta\right], \quad i = 1, 2 \tag{13}$$

where C_{ij} and D_{ij} are constants.

Then, inserting the above solutions into the boundary and interface conditions (2a) and (2b) leads to a homogeneous system of equations as

$$\mathbf{MX} = \mathbf{0} \tag{14}$$

Here, the 10×10 matrix $\mathbf{M}$ is a function of the material properties and the geometries of the interface edge. The explicit expressions of the matrix elements are listed in Shang and Kitamura (2003). The vector $\mathbf{X} = [A^1_{10}, B^1_{10}, A^1_{20}, B^1_{20}, A^1_{30}, B^1_{30}, C^2_{10}, D^2_{10}, C^2_{20}, D^2_{20}]^{\mathrm{T}}$. Eq. (14) has a nontrivial solution only if the determinant of $\mathbf{M}$ is zero, namely

$$\det \mathbf{M} = 0 \tag{15}$$

This equation thus governs the singularity order p in the stress field near the free edge along the interface Cr/PZT. By searching for the zeros of the determinant of the matrix $\mathbf{M}$, the singularity orders in the stress field near the free edge can be found.

From the above analyses, it can be concluded that the dominant term of the stress in the vicinity of the free edge of interface is in the form

$$\sigma_{ij} = \frac{K_{\mathrm{d}}}{r^{1-p}} f_{ij}(\theta) \tag{16}$$

Here, the singularity order is denoted by $1 - p$, K_{d} is the stress-intensity parameter, $f_{ij}(\theta)$ are angular functions.

4.3. Numerical results

The singularity order in the stress field near the free edge along the interface Cr/PZT is obtained by solving the eigenequation (15) numerically. Also, finite element analysis is carried out to verify the results.

In this study, ABAQUS code was used for the piezoelectric analysis. The material constants employed in all the computations are given in Tables 4–6 (Ikeda, 1996; Kanno et al., 1997).

The results of the stress singularity order for the Cr/PZT interface edge are summarized in Table 7. Numerical calculations show that Eq. (15) may have complex and several zeros in the open strip $0 < \mathrm{Re}(p) < 1$ for the edge geometry and material combinations. Table 7 includes only the p that has the smallest real part, which accordingly signifies the strongest singularity order of the stress field. It is found by theoretical solution that the singularity order of the normal stress, σ_z, for the interface edge Cr/PZT is 0.334, which is a strong singularity order, in comparison with the case of Pt/Ti, $\leqslant 0.02$.

Fig. 6 displays the distribution of the normal stress σ_z near the free edge along the interface Cr/PZT. The magnitudes of the stresses are normalized as σ_z/σ_0, where $\sigma_0 = P_d/S$ and S is the bonded area of the interface between the Cr and PZT films. It is observed that the tensile stress concentrates near the left edge of the interface. Furthermore, the stress distribution in the vicinity of the edge is nearly linear in the double-logarithmic scales. The slope of the linear part of the stress distribution signifies the existence of singularity in the stress field. The theoretical estimation of the singularity order is placed into the figure as well. It is shown that the numerical result is close to the theoretical one, as also seen in Table 7, where the numerical result was extracted from the slope of the stress–distance curve. Since the slope is dependent on the range of data included in a fitting procedure, the singularity order obtained from the FEM result is given as an approximate value. In addition, it is observed that the singular stress governs only the local region in the vicinity of the free edge along the interface Cr/PZT.

Table 4
Elastic stiffness (×GPa)

Material	c_{11}	c_{12}	c_{13}	c_{33}	c_{44}
PZT	114.254	58.294	58.525	98.181	20.75
Cr	Young's modulus $E = 279.24$ GPa, Poisson's ratio $v = 0.21$				

Table 5
Piezoelectric constants (C/m^2)

Material	e_{15}	e_{31}	e_{33}
PZT	10.249	−3.0822	10.9501

Table 6
Dielectric permittivities ($\times 10^{-9}$ F/m)

Material	ϵ_{11}	ϵ_{33}
PZT	5.4187	3.5328

Table 7
Singularity order $1-p$ of piezoelectric interface edge

	Theoretical result	FEM result
Cr/PZT	0.334	0.32–0.35

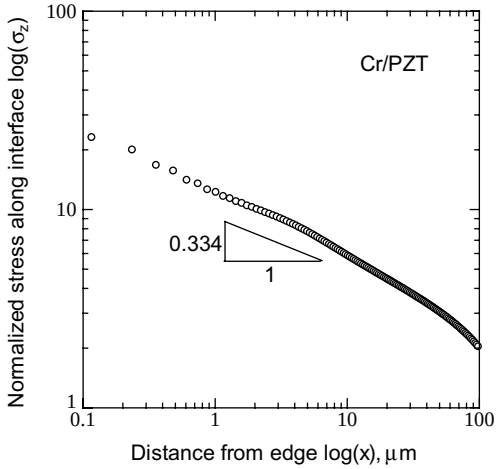

Fig. 6. Normal stress distribution near the free edge along Cr/PZT interface.

5. Interface toughness

It is well accepted that fracture mechanics approach applies to the evaluation of material toughness by employing the concept of stress intensity factor. Moreover, the experimental results for other thin film materials justified that the criterion of interface crack initiation could be prescribed by analogous stress intensity parameter (Kitamura et al., 2003; Hirakata, 2003). For the interface edge Cr/PZT considered here, a delamination criterion involving K_d is adopted to estimate the interface toughness for crack initiation at the free edge along the interface Cr/PZT,

$$K_d \geqslant K_{dc} \tag{17}$$

The critical stress intensity parameter at the delamination load, K_{dc}, is calculated by the FEM analysis, and the magnitude is summarized in Fig. 7. The interface toughness at the free edge along Cr/PZT interface can be determined as $2.206 \pm 0.27\,\mathrm{MPa\,m^{0.334}}$. It should be emphasized that the interface toughness K_{dc}

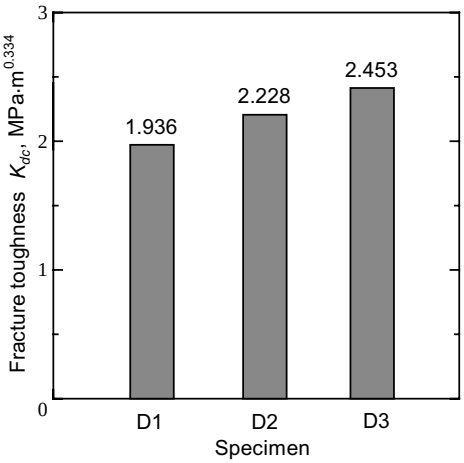

Fig. 7. Fracture toughness at the free edge of Cr/PZT interface.

adopted here is different with the fracture toughness for a body with pre-existing crack, and this interface toughness characterizes the resistance of the film/substrate system against the delamination initiation at the free edge along the interface.

6. Conclusions and future work

The interface strength of the PZT thin films deposited on silicon substrate has been investigated experimentally and theoretically in this work. The focus is put on crack initiation from the free edge along the interface. At first, the piezoelectric thin films with a sequence of Cr/PZT/PLT are deposited on Pt/Ti/Si substrates by magnetron sputtering technique. Then, the delamination tests are performed by utilizing the novel sandwiched cantilever specimen. The validity of this method is shown for the PZT thin films. The experimental results reveal that the delamination initiates at the free edge along the interface Cr/PZT and the abrupt cracking process is brittle of nature. These indicate that strong stress intensification prevails over the region near the free edge and the delamination is controlled by a parameter like stress-intensity factor. Therefore, the second part of this study is devoted to a theoretical analysis for the stress field near the free edge along the interface Cr/PZT, and the stress singularity order is found to be around 0.334, which is relatively strong. Based on these results, a delamination criterion involving the stress intensity parameter K_d is adopted to estimate the interface toughness for crack initiation at the free edge along the interface Cr/PZT. It is proved that the crack initiation is governed by the critical stress intensity parameter at the delamination load K_{dc}. The criterion of interface crack initiation is evaluated as $K_{dc} = 2.206\,\mathrm{MPa\,m}^{0.334}$.

In summary, the current study mainly targeted and discussed the crack initiation at the interface edge of the piezoelectric thin films, and the specimen adopted was designed for the crack initiation test. As a further consideration, the behavior of the interfacial crack growth of the piezoelectric thin films must be understood as well. To this end, several future works might be suggested as follows: (1) the interfacial crack growth tests should be conducted using sandwich delamination specimens (see a review article by Hutchinson and Suo, 1992) or newly designed specimens (e.g., Arai et al., 2003); (2) the solutions for the interfacial cracks in multilayered piezoelectric thin films should be worked out, or they are obtainable in the literatures (see review articles by Zhang et al., 2002; Chen and Lu, 2003); (3) based on these developments, correlation between the interface toughness for crack initiation and crack growth of the piezoelectric thin films could be investigated.

Acknowledgments

This work was supported by the Japan Society for the Promotion of Science (JSPS) and by the Center of Excellence for Research and Education on Complex Functional Mechanical System (COE Program of the Ministry of Education, Culture, Sports, Science and Technology, Japan). The authors wish to gratefully acknowledge the collaboration with S. Kinoshita on AES measurements. The authors also wish to thank Dr. Y. Umeno for fruitful discussions, K. Ohishi and M. Yokoyama for help with delamination tests.

Appendix A. Expressions for the matrices and vectors in Section 4

Here, we give the expressions of the matrices and the vectors appeared in Section 4:

$$\mathbf{A} = \begin{bmatrix} \cos^2\theta & \sin^2\theta & \sin 2\theta \\ \sin^2\theta & \cos^2\theta & -\sin 2\theta \\ -\sin\theta\cos\theta & \sin\theta\cos\theta & \cos 2\theta \end{bmatrix} \tag{A.1}$$

$$\mathbf{B}_1 = \begin{bmatrix} c_{11} & c_{13} & 0 & 0 & e_{31} \\ c_{13} & c_{33} & 0 & 0 & e_{33} \\ 0 & 0 & c_{44} & e_{15} & 0 \end{bmatrix} \tag{A.2}$$

$$\mathbf{B}_2 = \begin{bmatrix} 0 & 0 & e_{15} & -\epsilon_{11} & 0 \\ e_{31} & e_{33} & 0 & 0 & -\epsilon_{33} \end{bmatrix} \tag{A.3}$$

$$\mathbf{C} = \begin{bmatrix} \cos\theta & 0 & 0 & -\sin\theta & 0 & 0 \\ 0 & \sin\theta & 0 & 0 & \cos\theta & 0 \\ \sin\theta & \cos\theta & 0 & \cos\theta & -\sin\theta & 0 \\ 0 & 0 & \cos\theta & 0 & 0 & -\sin\theta \\ 0 & 0 & \sin\theta & 0 & 0 & \cos\theta \end{bmatrix} \tag{A.4}$$

$$\mathbf{D} = \begin{bmatrix} \cos\theta & \sin\theta \\ -\sin\theta & \cos\theta \end{bmatrix} \tag{A.5}$$

$$\mathbf{E}_i = \begin{bmatrix} \cos\theta & -\sin\theta \\ k_{1i}\sin\theta & k_{1i}\cos\theta \\ k_{2i}\sin\theta & k_{2i}\cos\theta \end{bmatrix} \tag{A.6}$$

$$\mathbf{\Lambda}_{1i}^{\mathrm{T}} = \left(\psi_{i,rr}, \left(\frac{\psi_{i,\theta}}{r} \right)_{,r} \right) \tag{A.7}$$

$$\mathbf{\Lambda}_{2i}^{\mathrm{T}} = \left(\frac{\psi_{i,r\theta}}{r}, \frac{\psi_{i,\theta\theta}}{r^2} \right) \tag{A.8}$$

$$\mathbf{B}_3 = \frac{1}{2\mu} \begin{bmatrix} \lambda + 2\mu & \lambda & 0 \\ \lambda & \lambda + 2\mu & 0 \\ 0 & 0 & 2\mu \end{bmatrix} \tag{A.9}$$

In (A.2) and (A.3), c_{ij}, e_{ij}, ϵ_{ij} are the elastic, piezoelectric and dielectric constants of piezoelectric material, respectively. λ, μ in (A.9) are Lamé constants of elastic material.

References

Arai, M., Okajima, Y., Kishimoto, K., 2003. Coating interface fracture toughness evaluation by a combination of edge compression and slinging load. In: Proceedings of the Fifth International Conference on Fracture and Strength of Solids, FEOFS, Sendai, Japan.

Bogy, D.B., 1968. Edge-bonded dissimilar orthogonal elastic wedges under normal and shear loading. Journal of Applied Mechanics 35, 460–466.

Bogy, D.B., 1971. Two edge-bonded elastic wedges of different materials and wedge angles under surface tractions. Journal of Applied Mechanics 38, 377–386.

Bubert, H., Jenett, H., 2002. Surface and Thin Film Analysis. Wiley-VCH Verlag, Weinheim.

Chen, Y.H., Lu, T.J., 2003. Cracks and fracture in piezoelectricsAdvances in Applied Mechanics, vol. 39. Academic Press, San Diego, pp. 122–215.

Ding, H.J., Chen, B., Liang, L., 1996. General solutions for coupled equations for piezo-electric media. International Journal of Solids and Structures 33, 2283–2298.

Evans, A.G., Hutchinson, J.W., 1995. The thermo-mechanical integrity of thin films and multilayers. Acta Metallurgical Materials 43 (7), 2507–2530.

Gardeniers, J.G.E., Verholen, A.G.B.J., Tas, N.R., Elwenspoek, M., 1998. Direct measurement of piezoelectric properties of sol–gel PZT films. Journal of Korean Physical Society 32, S1573–1577.

Hein, V.L., Erdogan, F., 1971. Stress singularities in a two-material wedge. International Journal of Fracture Mechanics 7 (3), 317–330.

Hirakata, H., 2003. Mechanical study on the delamination strength of interface between thin film and substrate. Ph.D. Thesis, Kyoto University, Japan.

Hutchinson, J.W., Suo, Z., 1992. Mixed mode cracking in layered materialsAdvances in Applied Mechanics, vol. 29. Academic Press, San Diego, pp. 64–191.

Ikeda, T., 1996. Fundamentals of Piezoelectricity. Oxford University Press, Oxford.

Kanno, I., Fujii, S., Kamada, T., Takayama, R., 1997. Piezoelectric properties of *c*-axis oriented $Pb(Zr,Ti)O_3$ thin films. Applied Physics Letters 70, 1378–1380.

Kanno, I., Fujii, S., Kamada, T., Takayama, R., 1998. Piezoelectric characteristics of *c*-axis oriented $Pb(Zr,Ti)O_3$ thin films. Journal of Korean Physical Society 32, S1481–1484.

Kanno, I., Kotera, H., Wasa, K., Matsunaga, T., Kamada, T., Takayama, R., 2003. Crystallographic characterization of epitaxial $Pb(Zr,Ti)O_3$ films with different Zr/Ti ratio grown by radio-frequency-magnetron sputtering. Journal of Applied Physics 93 (7), 4091–4096.

Kinbara, A., Kusano, E., Kamiya, T., Kondo, I., Takenaka, O., 1998. Evaluation of adhesion strength of Ti films on Si(100) by the internal stress method. Thin Solid Films 317, 165–168.

Kitamura, T., Shibutani, T., Ueno, T., 2002. Crack initiation at free edge of interface between thin films in advanced LSI. Engineering Fracture Mechanics 69, 1289–1299.

Kitamura, T., Hirakata, H., Itsuji, T., 2003. Effect of residual stress on delamination from interface edge between nano-films. Engineering Fracture Mechanics 70, 2089–2101.

Lane, M.N., Krishna, N., Hashim, I., Dauskardt, R.H., 2000. Adhesion and reliability of copper interconnects with Ta and TaN barrier layers. Journal of Materials Research 15, 203–211.

Lee, S.H., Jeon, M.S., Hong, K.I., Lee, J.W., Kim, C.K., Choi, D.K., 2000. Cantilever type lead zirconate titanate microactuator utilizing ruthenium oxide. Japanese Journal of Applied Physics 39, 2859–2862.

Lee, C.S., Jin, W.H., Nam, H.J., Cho, S.M., Kim, Y.S., Bu, J.U., 2003. Micro cantilevers with integrated heaters and piezoelectric detectors for low power SPM. In: Proceedings of the Sixteenth Annual International Conference on Micro Electro Mechanical Systems. IEEE, Kyoto, Japan.

Li, Y., Sato, Y., Watanabe, K., 2002. Stress singularity analysis of axisymmetric piezoelectric bonded structure. JSME International Journal Series A 45 (3), 363–370.

Muralt, P., Kholkin, A., Kohli, M., Maeder, T., 1996. Piezoelectric actuation of PZT thin-film diaphragms at static and resonant conditions. Sensors and Actuators A (Physical) 53 (1–3), 398–404.

Muralt, P., 1997. Piezoelectric thin films for MEMS. Integrated Ferroelectrics 17, 297–305.

Ramesh, R., 1997. Thin Film Ferroelectric Materials and Devices. Kluwer, Boston.

Scott, J.F., Araujo, C.A., 1989. Ferroelectric memories. Science 246 (4936), 1400–1405.

Shang, F., Kuna, M., Abendroth, M., 2003. Finite element analyses of three-dimensional crack problems in piezoelectric structures. Engineering Fracture Mechanics 70, 143–160.

Shang, F., Kitamura, T., 2003. On the modeling of stress singularity at the interface edge between piezoelectric thin film and elastic substrate. In: Proceedings of the 2003 JSME-IIP/ASME-ISPS Joint Conference on Micromechatronics for Information and Precision Equipment. JSME/ASME, Yokohama, Japan.

Timoshenko, S.P., Goodier, J.N., 1987. Theory of Elasticity, third ed. McGraw-Hill, Tokyo.

Volinsky, A.A., Tymiak, N.I., Kriese, M.D., Gerberich, W.W., Hutchinson, J.W., 1999. Quantitative modeling and measurement of copper thin film adhesion. Material Research Society Symposium 539, 277–290.

Wang, Z., Zheng, B., 1995. The general solution of three-dimensional problems in piezo-electric media. International Journal of Solids and Structures 32, 105–115.

Williams, M.L., 1952. Stress singularities resulting from various boundary conditions in angular corners. Journal of Applied Mechanics 19, 526–528.

Xu, J.Q., Mutoh, Y., 2001. Singularity at the interface edge of bonded transversely isotropic piezoelectric dissimilar materials. JSME International Journal Series A 44, 556–566.

Zhang, T.Y., Zhao, M.H., Tong, P., 2002. Fracture of piezoelectric ceramicsAdvances in Applied Mechanics, vol. 38. Academic Press, San Diego, pp. 148–290.